

# **CHAPTER 3:**

**Fabrication of AChE biosensor through electroentrapment in polypyrrole and optimisation**

### 3.1 Introduction

Effective immobilization of enzyme to solid electrode surface still remains as a great challenge for the fabrication of biosensor. A key consideration for immobilizing enzyme is how to retain its bioactivity. The usual immobilization methods include direct physical adsorption on a solid support<sup>1</sup>, cross linking<sup>2</sup>, encapsulation into a hydro gel<sup>3</sup>, covalent binding<sup>4,5</sup>, entrapment in different substrate materials<sup>6,7</sup>, self-assembly into multilayer film<sup>8</sup>, immobilization on controlled-pore glass<sup>9</sup> and immobilization on magnetic particles<sup>10</sup>. The conducting polymers have attracted much attention due to their interesting electrical and electrochemical properties<sup>11,12</sup> and also due to their potential application in miniaturized electronic devices. Polypyrrole (PPy), a key member of the organic conducting polymers, has been widely used as the enzyme- hosting matrix in electrochemical biosensors due to its advantages of permitting a facile electronic charge flow through the polymer matrix, easy preparation, high conductivity and good stability<sup>13</sup>. In these PPy based biosensors the enzyme was either electro entrapped inside the PPy matrix or attached to the surface of PPy film in pure or composite form. These include electro entrapment of glucose oxidase (GOX)<sup>14,15</sup> for glucose determination, electro entrapment of tyrosinase for determination of phenolic compounds<sup>16</sup>, surface attachment of acetylcholinesterase (AChE) on PPy and polyaniline (PANI) composite polymer film doped with multi-walled carbon nanotube<sup>4</sup> and on Au nanoparticles-polypyrrolenano wire composite film<sup>17</sup> for determination of OP and OC pesticides. Though the surface immobilized PPy-AChE-nanomaterial sensors can give high sensitivity, their durability is poor due to bio-fouling and washing out of the enzyme. Moreover the fabrication processes are very much cumbersome and expensive due to involvement of multiple chemical steps and costly chemicals such as the nanoparticles. Electro entrapment procedures are easy, single step procedure and due to the encapsulation of the enzyme by the macromolecular matrix, the enzyme is better protected from washing out during analytic application of the sensor and hence expected to be more durable compared to the surface immobilized AChE sensors. This approach may help in imparting selectivity to the enzyme biosensors through control of the film porosity. Also, since polypyrrole film is not easily degraded by some of the organic solvents, therefore, such an approach may pave the way for real sample analysis in organic phase. To our knowledge so far no work has been reported that has documented the use of electro entrapped AChE for pesticide sensing.

### 3.2 Objectives

1. AChE will be immobilized through electroentrapment using electrochemical chronoamperometric method. Cross linker glutaraldehyde be used to prevent enzyme leaching. Biocompatible microenvironment inside the polypyrrole matrix for the enzyme will be created through the use of gelatin.
2. Immobilization will be confirmed through SEM and electrochemical study.
3. Electrochemical behavior of polypyrrole entrapped AChE will be studied.
4. Optimum amount of supporting electrolyte (KCl) during film deposition that is necessary for biosensor stability will be identified and applied.
5. Optimization of operational conditions for maximum signal output will be done by evaluating the saturated substrate concentration, maximum enzyme loading and optimum pH.
6. Suitable reactivation mechanism will be worked out for reuse of the sensor.
7. Optimum composition of organic solvent for biosensor functioning will be found out.
8. Finally the sensor will be applied for analysing test samples of OP and OC pesticides.

### 3.3 Experimental

#### 3.3.1 Preparation of the sensor

The sensor probe was prepared by immobilizing AChE at the tip of a platinum (Pt) electrode (2 mm) with PPy as the support matrix. The Pt electrode was cleaned by polishing with fine alumina powder followed by sonicating for 15 minutes. For electro deposition 2 mL of 0.5 M pyrrole solution in phosphate buffer (pH 7.2) containing 0.02M KCl and 5  $\mu\text{L}$  ( $100 \text{ U mL}^{-1}$ ) of the enzyme were mixed together in a three electrodes cell set up comprised of platinum working electrode, platinum coil auxiliary electrode and Ag/AgCl saturated with 3M NaCl as the reference electrode. Electrolysis was carried out at 0.8 V for 30 minutes. Before starting the electrolysis, the solution mixture was sonicated for 5 minutes. A thick film of PPy-AChE was developed at the tip. The film was then washed with phosphate buffer saline (PBS) (pH 7.2) and dried at room temperature for 30 minutes. Then, holding the electrode vertical, with its film containing end upwards, 5  $\mu\text{L}$  of 5% gelatin solution ( prepared by warming gelatin

water mixture up to 60 °C followed by cooling down to room temperature) was added to it and then kept at room temperature for 1 hour. Then glutaraldehyde (35% in water) was added in two steps. At first, 5 µL glutaraldehyde was added to the electrode tip with a micro syringe, keeping the electrode vertical. The electrode was then kept at room temperature in the same vertical position until the film appeared dry (for approximately 1 h). Then the electrode tip was again treated with glutaraldehyde by immersing it in the stock solution (35%) for 1 min. The electrode was then kept at room temperature for 4 hours followed by overnight storage at 0 °C. Finally it was transferred to a -20 °C freezer where it was stored for 5 days before use.

### 3.3.2 Measurement procedure

Quantitative estimation of sensor response was done mostly through chronoamperometric (CA) method, but cyclic voltammetry (CV) was also applied in few cases. The cell set up comprised of three electrodes, the sensor probe as working, Pt coil as auxiliary and Ag/AgCl saturated with 3M NaCl as reference electrodes in PBS (pH 7.2) electrolyte. Initial voltage  $E_0 = 0.0$  V was applied for 60 seconds, final potential  $E = 0.70$  V for 400 seconds and ATChCl was added at 300s, i.e., after sufficient current stabilization. After taking out from -20 °C freezer, prior to its application, the sensor was soaked in PBS for 30 minutes and then potentiostated at 0.8 V for 15 minutes. The experiments were performed at 32 °C with constant magnetic stirring. Triplicate measurements were made in all experiments, with four cycles of potential sweep for the CVs, unless stated otherwise.

Time dependence of the inhibitory action of the pesticides was studied by evaluating the percent residual activity ( $\%A_r$ ) with time and the concentration dependence of the same was studied by evaluating the relative inhibition percentage ( $I$  %) with concentrations, using respectively Eq.2.1 and Eq.2.2

### 3.4 Results and discussion

#### 3.4.1 Confirmation of immobilization

##### 3.4.1.1 SEM

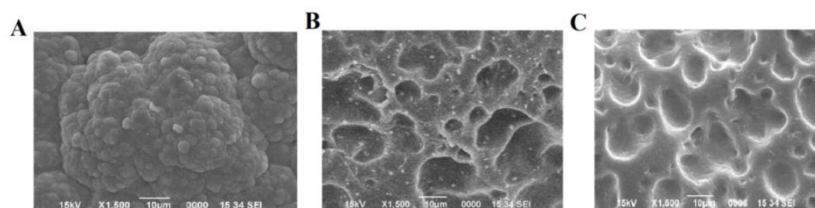


Fig.3.1 SEM images of (A) PPy film (B) AChE doped PPy film (C) PPy-AChE-Geltn<sup>1</sup>-Glut<sup>2</sup> film.

The morphology of PPy film, PPy-AChE, and PPy-AChE-Geltn-Glut electrode were characterized by SEM as shown in Fig.3.1. Electrodeposited PPy film showed a granular morphology (A). Electrodeposition from a sonicated mixture of the pyrrole and enzyme resulted into a film with compact growth pattern and uniformly distributed enzyme units (B). In Fig.3.1C, the gelatin-glutaraldehyde layer is seen covering the scattered enzyme units.

#### 3.4.2 Electrochemical (CV) behavior towards thiocholine oxidation

Fig.3.2 shows the typical cyclic voltammograms (CVs) of the sensor and the immobilization matrix towards thiocholine oxidation at scan rate 20 mV/s. When CV was performed with the sensor in ATChCl, three peaks were seen (Curve 'b'). That these peaks were due to enzyme-substrate interaction only, is clear from a comparison of curve 'b' with curve 'c' (Pt-PPy-AChE-Geltn-Glut in PBS) and curve 'd' (Pt-PPy-Geltn-Glut in ATChCl). That none of these peaks is due to interaction of ATChCl with bare platinum electrode or PPy modified platinum electrode is obvious from curve 'f' and curve 'g' which are respectively the CVs of bare platinum electrode and polypyrrole coated platinum electrode in 2.0 mM ATChCl. That electro oxidation of gelatin and /or glutaraldehyde is not behind these peaks, is obvious from curve 'e', where the same three peaks appeared in absence of them.

Seen in the inset (Fig.3.2) are those three peaks. One intense anodic peak (A) at 0.80 V (RSD 0.26% and peak current 605  $\mu$ A with RSD 0.12%), one intense cathodic peak (B) at -0.65 V

(RSD 0.3% and peak current 532.7  $\mu\text{A}$  with RSD 0.44%) and a low intensity anodic peak (C) at -0.30 V to 0 V region.

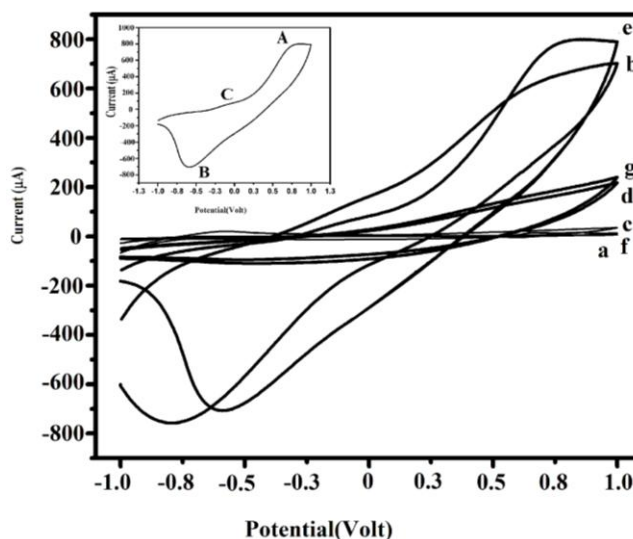


Fig.3.2 Cyclic voltammograms at scan rate 20 mV/s of (a) Pt electrode in PBS (b) sensor in 2.0 mM ATChCl (c) sensor in PBS (d) Pt-PPy-Geltn-Glut electrode in 2.0 mM ATChCl(e) Pt-PPy-AChE electrode in 2.0 mM ATChCl. (f) Pt electrode in ATChCl (g) Pt-PPy electrode in 2.0 mM ATChCl. *Inset: Fig. 3.2e.*

Intensity of both the peaks A and B found to vary with ATChCl concentration, although their trends of variation were not same. Variation of A with ATChCl followed Michaelis - Menten plot characteristic. So it is attributed to be oxidation of TCh produced during enzymatic hydrolysis of ATChCl. Variation of peak B was nonlinear initially but showed Michaelis-Menten plot characteristic when few initial values were discarded during continuous CV run in same ATChCl solution using the enzyme electrode. It indicates the possibility of occurring of two reduction processes at -0.65 V, one of which might be the reduction of RSSR formed during anodic oxidation of ATChCl. Peak C tends to disappear at low scan rate i.e., when relatively more enzyme substrate contact time is allowed. So it is probably due to some slow reaction between PPy surface and unhydrolyzed acetylthiocholine (ATCh).

The effects of scan rate on the cyclic voltammetric behavior of the sensor are shown in Fig.3.2

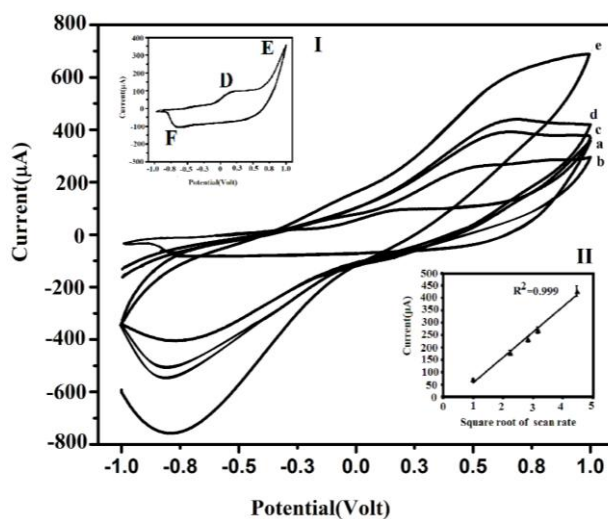


Fig.3.3 Cyclic voltammograms of the sensor in 2.0 mM ATChCl at different scan rates.(a) 1 mV/s (b) 5 mV/s (c) 8 mV/s (d) 10 mV/s (e) 20 mV/s. *Inset I*: Fig. 3.5.3a; *Inset II*: Scan rate vs. peak current.

The peak current found to increase and peak maxima shifted towards more positive potential with increasing scan rate. Inset I (Fig.3.3) is curve 'a' which is the CV at 1 mV/s. Here two anodic peaks D (0.20V, RSD 0.35%, 71.2  $\mu$ A, RSD 0.32%) and E (from 0.65 V onwards, with RSD1.5%), and one cathodic peak F (-0.60V, RSD 0.20%, 124.1  $\mu$ A, RSD 0.80%) are seen. With increasing scan rate peak D shifted to the higher potential side and got merged with peak E at a scan rate of about 8 mV/s and at a potential of 0.60 V (RSD 0.17%, peak current 234.9  $\mu$ A with RSD 0.47%, Fig.3.3 Curve 'c'). With further increase in scan rate the peak maxima of both anodic and cathodic peaks got shifted further (0.80 V, 429.6  $\mu$ A with RSD 0.26% and 0.37% respectively; -0.80V, 409.7  $\mu$ A with RSD 0.21% and 0.51% respectively, Fig.3.3, curve 'e'). It indicates that both the peaks D and E, originated from the electro oxidation of the same species- thiocholine (further justification to this point comes from Fig.3.4) where peak current of D increases with increasing ATCh concentration. Peak F is same as the cathodic peak of Fig.3.3b, which appears due to reduction of the di-thio species. It has been attributed that peak D appears due to oxidation of thiocholine ions those diffuse into the PPy matrix, whereas peak E is due to oxidation of thiocholine ions in the solution at the vicinity of the PPy surface. Peak currents measured from the base line of charging current, was found to be linear with the square root of the scan rate which indicates

a diffusion controlled electrochemical process (inset II, Fig.3.3). As seen in the Fig.3.3 (Curve 'a'), the thiocholine oxidation peak appeared at 0.20 V when a completely fabricated electrode was used, the same was obtained at 0.10V (RSD 0.69% and peak current 103.8  $\mu\text{A}$  with RSD 0.19%) with a freshly prepared Pt-PPy-AChE electrode (Fig.3.4). The reason probably is, when the PPy surface is coated with gelatin and gluteraldehyde the diffusion of thiocholine ions to PPy matrix get hindered and become slower, which causes the oxidation peak to shift towards the higher potential side.

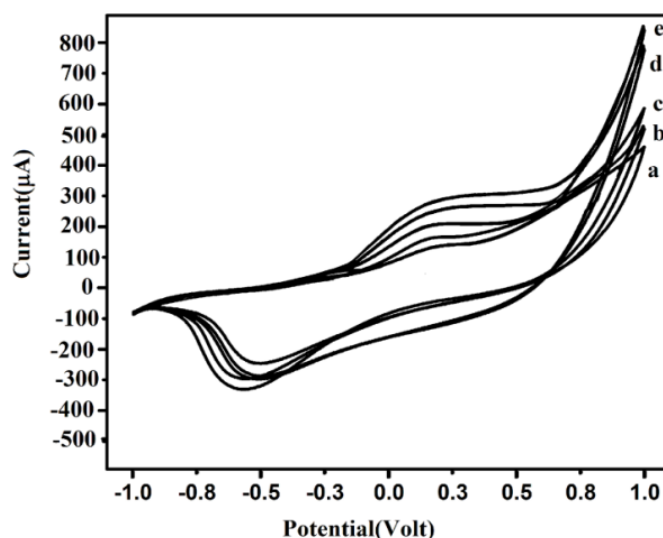


Fig.3.4 Cyclic voltammograms of Pt-PPy-AChE electrode in varying amount of ATChCl at scan rate 1 mV/s, in the potential range from -1 V to 1 V. (a) 50  $\mu\text{L}$  (b) 100  $\mu\text{L}$  (c) 150  $\mu\text{L}$  (d) 200  $\mu\text{L}$  (e) 250  $\mu\text{L}$ . ATChCl stock solution 0.020 M, cycle sweep 3.

Thus, it is inferred that thiocholine electro oxidation in PPy occurs at 0.1 V. This potential is much lower than the oxidation potential of 0.70V of thiocholine on solid electrodes, as reported in literature (Liu et al., 2005).<sup>18</sup> The enhancement of the amperometric signal and lowering of the oxidation potential are attributed to be due to its inherent conductivity and electro catalytic property of PPy. It is noteworthy to mention that, although the thiocholine oxidation in presence of PPy occurs at 0.1 V, a potential of 0.7 V was used during chronoamperometric analysis so that the sensitivity is maximum.



### 3.4.3 Enzyme leaching test

Ellman's spectrophotometric experiment<sup>19</sup> was performed to check if any trace amount of enzyme can leach out from the immobilization matrix during electrochemical treatment of the sensor. This was done by performing more than 40 blank CV and CA runs with the prepared sensor, taking phosphate buffer saline (PBS) as the electrolyte followed by subjecting the same electrolyte to Ellman's spectrophotometric test at 412 nm. Assay was prepared by adding ATChCl and DTNB to the PBS solution in the UV cuvette but not the enzyme. No increase in absorption with time was observed, indicating that, the enzyme units can't leach out from the sensor during the electrochemical treatment.

### 3.4.4 Optimum concentration of supporting electrolyte KCL during film deposition

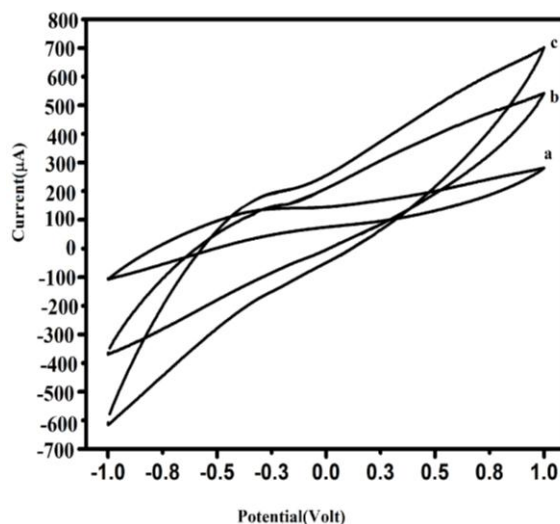


Fig.3.5 Cyclic Voltammetric behaviour of the chloride doped PPy film towards 2.0 mM ATChCl. (a) Doped with 0.02 M KCl (b) doped with 0.05 M KCl (c) doped with 0.1 M KCl.

The effect of KCl quantity during electro deposition of PPy on signal intensity and sensor operational stability was studied in the range 0.02 to 0.1M KCl using cyclic voltammetry. At higher KCl concentration, film formation was found to be easier but the film thus formed showed higher background current and lower signal reproducibility during analytical application. The increase of the background current at higher chloride doping is probably due to the potential response behavior of the film as reported in the literature.<sup>20,21</sup>

The instability in the amperometric signal with number of measurements at higher chloride doping is probably due to leakage of chloride ions, which in turn affects the background

current, as is obvious from Fig.3.5 To minimize the artificial increase in the sensor signal and also to have better stability, a lower amount of KCl (0.02M) was used during electro deposition of the film.

### 3.4.5 Optimization of the fabrication process

#### 3.4.5.1 Saturated substrate concentration

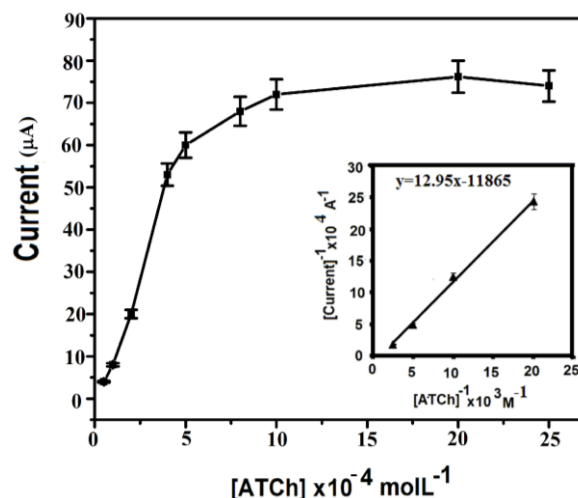


Fig.3.6 Variation of sensor response with substrate concentration when the enzyme loading was 0.5U. *Inset*: Lineweaver -Burk plot for determination of  $K_m^{app}$ .

The saturated substrate concentration of acetylthiocholine was determined through the Michaelis-Menten plot (Fig.3.6) and found to be 2.0 mmol L<sup>-1</sup>. The apparent Michaelis-Menten constant,  $K_m^{app}$  was evaluated through chronoamperometry method found to be 1.09 mmolL<sup>-1</sup>, which was calculated from the lower linear part of the Michaelis-Menten plot (inset, Fig.3.6), following the Lineweaver-Burk equation (Eq.3).

$$\frac{1}{i} = \frac{1}{i_{\max}} + \frac{K_m^{app}}{i_{\max}} \frac{1}{[ATCh]} \quad (3.1)$$

Here  $i_{\max}$  corresponds to the saturation current of thiocholine oxidation.

This value of apparent Michaelis-Menten constant ( $K_m^{app}$ ) is in the range of the values reported by other authors: for AChE adsorbed on polyethyleneimine modified electrode the result is 1.5 mmolL<sup>-1</sup> obtained by Vakurov et al.<sup>22</sup> and for AChE adsorbed on screen-printed carbon electrode covered with Prussian Blue and Nafion the value was  $0.84 \pm 0.44$  mmolL<sup>-1</sup> reported by Suprun et al.<sup>23</sup> The thiocholine sensitivity of the PPy-AChE-Gel-Glu sensor was

calculated from the linear part of the Michaelis - Menten plot and was found to be 143 mA/M.

The apparent Michaelis-Menten constant ( $K_m^{app}$ ) of the free enzyme was also determined under the same experimental condition and found to be  $1.39 \text{ mmolL}^{-1}$  and the thiocholine sensitivity was 4 mA/M. The lowering of  $K_m^{app}$  value of the immobilized enzyme compared to free enzyme was probably due to creation of diffusion channels in the enzyme loaded film which helped fast oxidation of the analyte. The Michaelis - Menten plot for the kinetics of the free enzyme is shown in Fig .3.7

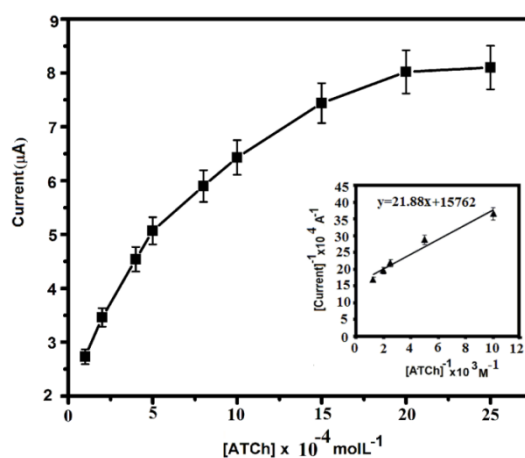


Fig.3.7 Variation of sensor response with substrate concentration measured in presence of externally added enzyme (0.5U). *Inset*: Lineweaver -Burk plot for determination of  $K_m^{app}$ .

#### 3.4.6 Effect of enzyme loading

To see the effect of enzyme loading, the enzyme was immobilized in PPy surface taking different quantities ranging from 1 to 50  $\mu\text{L}$  ( $100 \text{ UmL}^{-1}$ ) and their response to a fixed amount (2.0 mM) of acetylthiocholine chloride (ATChCl) were examined through cyclic voltammetry (Fig.3.8).

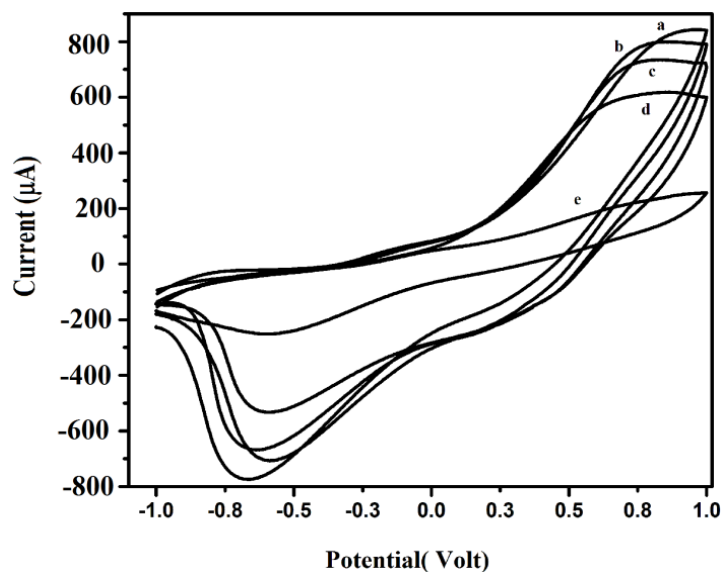


Fig.3.8 Effect of enzyme loading on sensor response when enzyme loading was (a) 1 $\mu$ L (b) 5  $\mu$ L (c) 10  $\mu$ L (d) 25  $\mu$ L (e) 50  $\mu$ L. Scan rate 20 mV/s.

From the cyclic voltammograms in Fig.3.8, it is obvious that the peak current decreases with increasing enzyme amount. The difference was not very significant between 1 and 5  $\mu$ L (0.1 to 0.5U) but significant decrease was seen from 5  $\mu$ L onwards. With a loading of 50  $\mu$ L enzyme, the peak almost disappeared. The decrease in peak is probably due to increasing diffusion limitation as reported in literature for PPy entrapped enzymes<sup>24</sup>. The peak potentials for curve 'b' through curve 'e' were found to be close to 0.80 V with a maximum relative standard deviation (RSD) of 0.26% while in curve 'a' it was 0.85 V with RSD 0.31%. Shift in peak potential in case of curve 'a' is probably due to reduction in the number of diffusion channels in the film.

#### 3.4.7 Effect of pH

The pH dependence of the enzyme electrode over the pH range 6.4 to 7.8 was studied through cyclic voltammetry. Fig.3.9 shows the cyclic voltammetric response of the sensor towards 2.0 mM ATChCl at different solution pH.

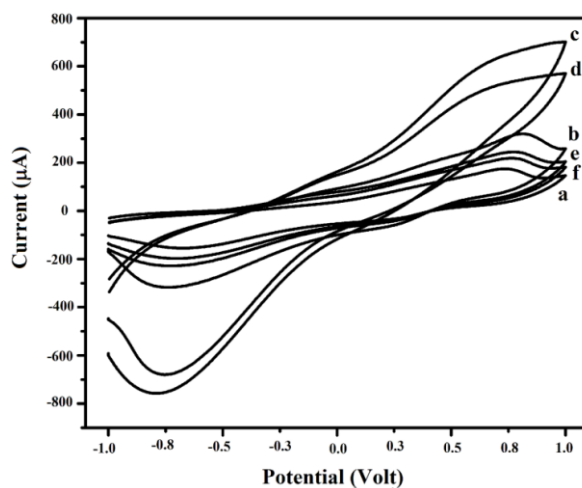


Fig.3.9 Effect of pH on the cyclic voltammetric behaviour of the sensor towards 2.0 mM ATChCl when enzyme loading was 0.5U, and scan rate 20 mV/s. (a) pH 7.8 (b) pH 7.4 (c) pH 7.2 (d) pH 7.0 (e) pH 6.8 (f) pH 6.4.

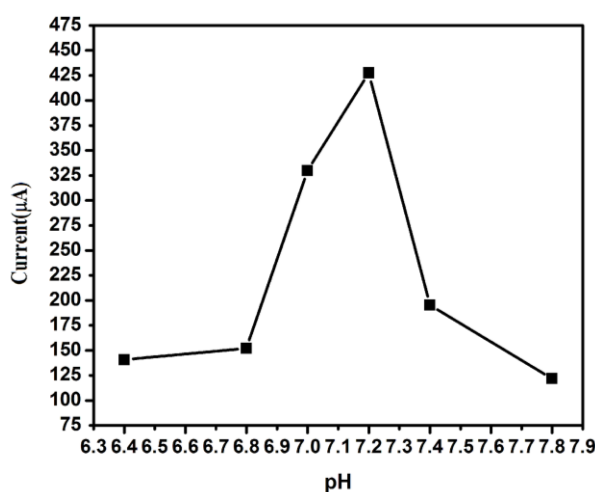


Fig.3.10 Plot of peak current versus solution pH.

The peak potentials and the base line corrected peak currents (with RSDs) found to be 0.80 V (0.31%), 121.8  $\mu$ A (0.73%), (pH 7.8); 0.85 V (0.20%), 195.4  $\mu$ A (0.56%), (pH 7.4); 0.80 V (0.24%), 427.6  $\mu$ A (0.37%), (pH 7.2); 0.80V (0.21%), 329.9  $\mu$ A (0.44%), (pH 7.0); 0.84 V (0.12%), 152.1  $\mu$ A (0.66%), (pH 6.8) and 0.83 V (0.17%), 140.8  $\mu$ A (0.53%), (pH 6.4). Variation in peak currents with the pH of the electrolyte is shown in Fig.3.10 It was found that the peak currents were higher near the biological pH (pH 7). The maximum value was obtained at pH 7.2. Thus it is clear that PPy does not alter the optimum pH for the catalytic behavior of cholinesterase.

### 3.4.8 Pesticide Inhibition study

#### 3.4.8.1 Effect on chronoamperometric signal

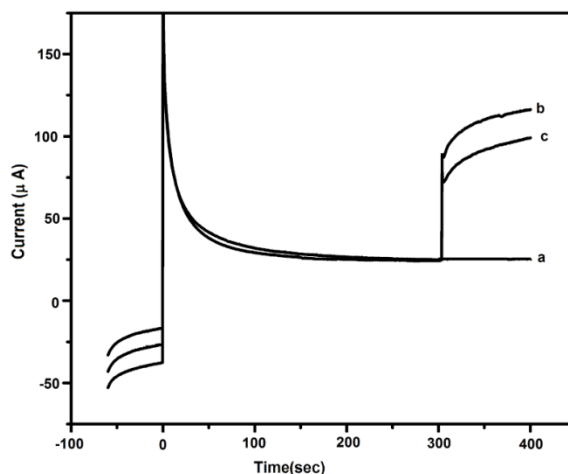


Fig.3.11 Chronoamperometric response of the sensor towards: (a) 200  $\mu\text{L}$  KCl (0.05 M) in PBS (b) 2.0 mM ATChCl (c) 2.0 mM ATChCl after incubation for 30 minutes in a 60 ppb paraoxon solution.

The effect of inhibition on the PPy-AChE-Gel-Glu sensor response was studied by examining the biosensor response to 2.0 mM ATChCl before and after incubation in inhibitor solution (Fig.3.11). Curve 'b' is the initial response of the sensor to 2.0 mM ATChCl and curve 'c' is the response after incubating the sensor in paraoxon solution for 30 min. The figure clearly indicates that, as a result of inhibition, amperometric response of the biosensor decreases. Response characteristic of the sensor towards sudden addition of inhibitor was studied for real time monitoring of inhibitor and shown in Fig.3.12

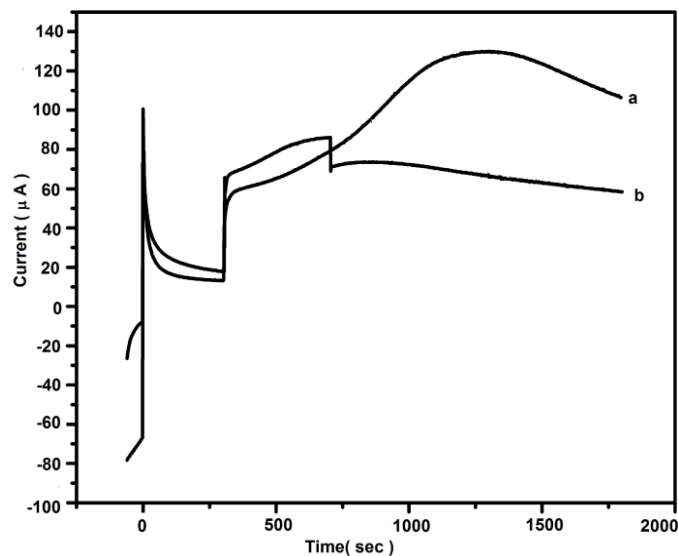


Fig.3.12 Real time monitoring of sensor response. (a) 2.0 mM ATChCl was added at 300s (b) 2.0 mM ATChCl at 300s followed by 200  $\mu$ L of 100 ppb paraoxon at 700s.

#### 3.4.8.2 Incubation time

The variation of residual activities of the biosensor with incubation time was studied for four differently concentrated inhibitor solutions each of paraoxon and carbofuran. Observing that carbofuran has stronger inhibitory effect than paraoxon. The concentration range 12.5, 60, 150 and 250 ppb for paraoxon and 5, 25, 60 and 100 ppb for carbofuran were selected for inhibition study. In each case the sensor was incubated for 1h duration and its response to 2.4 mM ATChCl and hence the percent residual activities were calculated by using Eq.2.1 (Fig.3.13).

We observed that, as compared to the other immobilization matrices used by different workers, relatively more time is required for AChE inhibition in presence of the thick PPy matrix used here. The reason probably is that, the inhibitor molecules need to overcome the diffusion barrier at first to cause effective inhibition.

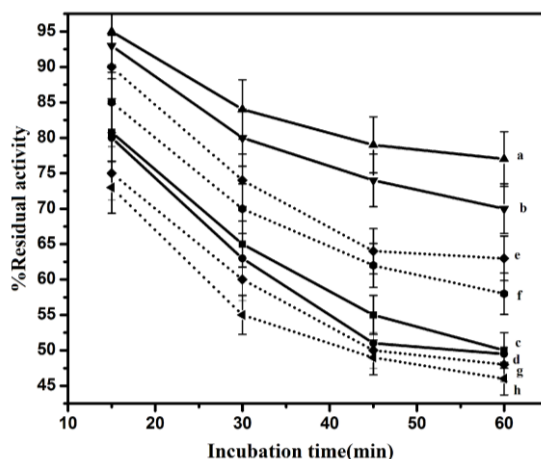


Fig.3.13 Effect of incubation time and concentration of inhibitor on the activity of the immobilized enzyme; bold lines (a) 12.5 ppb (b) 60 ppb (c) 150 ppb and (d) 250 ppb of paraoxon, dotted lines (e) 5 ppb (f) 25 ppb (g) 60 ppb and (h) 100 ppb of carbofuran.

#### 3.4.9 Enzyme reactivation studies

Enzyme reactivation studies were performed in both 2-PAM and 0.05 M NaF. That NaF can be effectively used for reactivation of the enzyme was known from the work of Kok et al.<sup>25</sup> In our study we have found that NaF is more effective reactivator than 2-PAM for AChE biosensor of this kind. The reason probably is that, due to its large sizes, the 2-PAM molecule cannot diffuse inside the gelatin-glutaraldehyde barrier to cause reactivation of the enzyme. On the contrary, due to their small size,  $F^-$  can diffuse easily and being a strong nucleophile, it can reactivate the enzyme. A 0.05M NaF was used for this purpose. The inhibited sensor was immersed in a solution of 0.05 M NaF for 15 minutes followed by washing and 15 minutes immersion in phosphate buffer (0.01M) solution. When the inhibition is less than 15 percent, 95-98% reactivation occurred. But when the percent inhibition is beyond 15 percent, reactivation decreased gradually.

#### 3.4.10 Reproducibility and stability

##### 3.4.10.1 Precision measurement

Inter-assay precision or the fabrication reproducibility of the sensor was confirmed by determining the response of six different fabrications to 2.0mM ATChCl solution. The relative standard deviation (RSD) of the measurements was calculated. A value of 6.56 % was obtained which indicates a good reproducibility of the fabrication process.



The intra state precision or the operational reproducibility was confirmed by evaluating the RSD of sensor response for six continuous CA run with a single fabrication, using 2.0 mM ATChCl. The RSD was found to be 0.742%, which indicates that the sensor response has acceptable precision for consecutive measurements of ATChCl.

#### 3.4.10.2 Operational Stability

The operational stability of the biosensor was confirmed by examining its repeated response to 2 mM ATChCl, both in absence and in presence of inhibitor. In absence of the inhibitor, the sensor signal was found to be stable for 40 continuous measurements. After 40 measurements, the signals showed decrease and dropped to 50% of its original value at the 60<sup>th</sup> measurement. To study the operational stability in presence of inhibitor, a 60 ppb solution each of paraoxon and carbofuran were used.

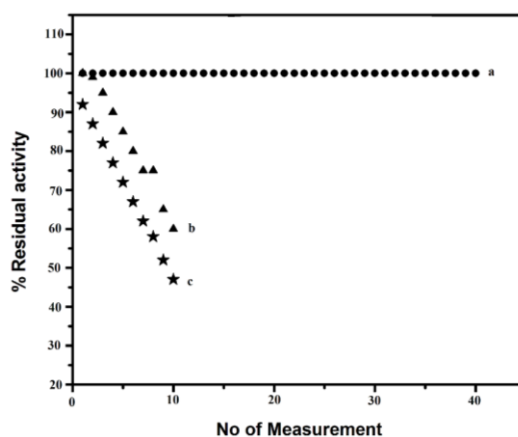


Fig.3.14 Repeated sensor response to 2.0 mM ATChCl (a) in absence of inhibitor (b) in presence of 60 ppb paraoxon solution (c) in presence of 60 ppb carbofuran solution.

It was observed that in presence of inhibitor, the percent residual activity ( $\%A_r$ ) of the enzyme decreased gradually and consequently the sensor signals got reduced to a value close to 60%, after 10 number of measurements, in case of paraoxon. In case of carbofuran the sensor response dropped down to 60% after 7th number of measurements. Fig.3.14 shows the response characteristics of the sensor in absence and presence of the inhibitors.

### 3.4.10.3 Storage stability

For evaluation of storage stability of the PPy-AChE-Gel-Glu sensor, a fresh fabrication was selected. After measuring the initial stable response, the sensor was stored at 0 °C and chronoamperometric responses were measured at the intervals of 30, 60, 90 and 120 days. No loss in enzyme activity was observed till 60 days. Slight decrease in the response was observed at 90 days and at the end of 120 days, 28% reduction in current signal was observed. To study the storage stability in wet condition, a freshly prepared sensor after initial treatment was immersed in phosphate buffer containing 0.05M KCl and kept at 4 °C for 120 days. No significant loss in enzyme activity was found at the end of 120 days. We noticed that the wet stored sensor showed relatively poor signal reproducibility as compared to the dry stored one when subjected to continuous analysis at the end of the stored period (120 days). The dry stored sensor gave stable value up to 36-40 measurements, whereas the wet stored sensor gave the same up to only 20 measurements. The reason probably is that, prolonged exposure to water/phosphate buffer medium results in some changes in the microenvironment of the PPy matrix that makes the sensor signal unstable. We have also studied the wet storage stability in Bovain Serum Albumin (BSA) solution in phosphate buffer, but no significant difference in the result was observed as compared to the phosphate buffer/ KCl case.

### 3.4.11 Optimum solvent for non aqueous application

Acetonitrile and ethyl acetate are the two solvents commonly used for extraction of pesticides from produce and have octanol water partition coefficient (logP) value respectively -0.33<sup>26</sup> and 0.68.<sup>26</sup> Having log P value less than 2 both solvents strongly deactivate the enzyme. However it has been established by different workers<sup>27</sup> that AChE activity remains unaffected in 5% acetonitrile. So we have tested the operational stability of prepared sensor in 5% acetonitrile. The sensor after measuring the initial response was incubated in 5% acetonitrile in PB at 32°C for three hours and response was determined at each 30 minutes interval. No decrease in sensor response was observed in Fig.3.15 which has proved that the prepared sensor can work well in 5% acetonitrile.

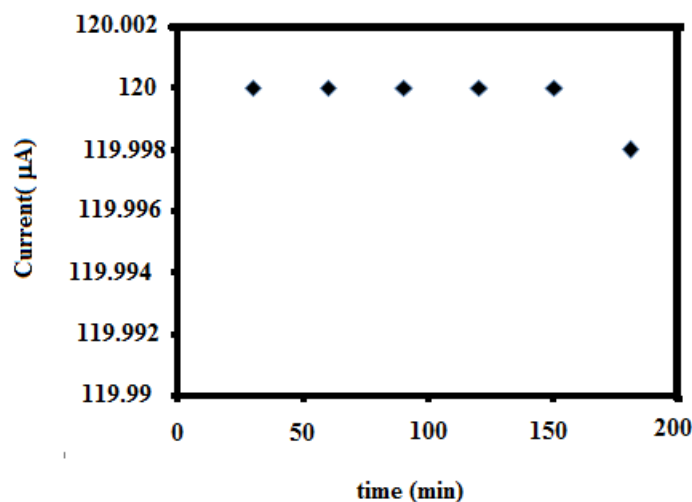


Fig.3.15 Sensor response to 2.0 mM ATChCl in presence of 5% acetonitrile in PBS at each 30 minutes interval.

### 3.4.12 Application to pesticide analysis and validation checking

#### 3.4.12.1 Calibration plot for pesticides

The calibration curves for paraoxon and carbofuran were obtained by plotting the percent relative inhibition ( $I$  %) (Eq.2.2) against concentrations, while allowing the incubation for 1 h. Paraoxon solutions were prepared in phosphate buffer while the carbofuran were in 5% acetonitrile. The calibration plots are shown in Fig.3.16 (A, B).

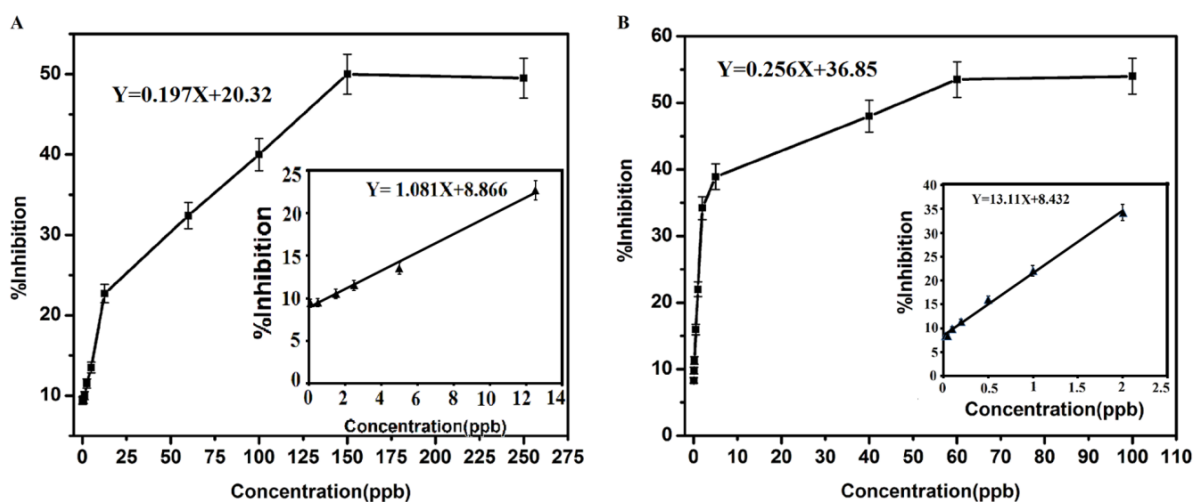


Fig.3.16 Calibration plot. (A) paraoxon in PB (B) Carbofuran in 5% acetonitrile. *Inset*: The expanded plot of the lower ranges.

In case of paraoxon the linear ranges were; from 0.1 ppb to 12.5 ppb ( $y = 1.081x + 8.866$ ,  $R^2 = 0.993$ ) and from 12.5 ppb to 150 ppb ( $y = 0.197x + 20.33$ ,  $R^2 = 0.998$ ). Maximum, but not complete, inhibition due to paraoxon occurred at 150 ppb, the amount of inhibition being 50%. In case of carbofuran the two linear ranges found were 0.025-2 ppb ( $y = 13.11x + 8.432$ ,  $R^2 = 0.998$ ) and 5-60 ppb ( $y = 0.256x + 36.85$ ,  $R^2 = 0.999$ ). Maximum inhibition occurred at 60 ppb with a value of 54%. Limit of detection ( $I_{10\%}$ ) were found to be 1.1 ppb and 0.12 ppb respectively for paraoxon and carbofuran. The difference of the linear range for the two pesticides could be attributed to the different degrees of pesticide inhibitions, which were caused by the different process of inhibition by the two pesticides. From the calibration curve it is obvious that the biosensor is more selective towards carbofuran than paraoxon. The ratios of the slopes of the two calibration curves in the two linear ranges are respectively 12.33 and 1.3 which indicates that carbofuran selectivity of the biosensor over paraoxon is more in the lower concentration range.

#### 3.4.12.2 Validation study

Biosensor validation was studied through analysis of tomato samples spiked with carbofuran and paraoxon. QuEChERS<sup>28</sup> extraction and clean up procedure was used in the work up step. 10 gram of tamato was fortified with 5 mL of 100 ppb solution of one of the pesticides. 10 gram of chopped vegetable (tamato) was spiked with 5 mL of standard pesticide solution (prepared in acetonitrile) and then homogenized. 5 mL of acetonitrile was added and shaken in vortex shaker for 5 minutes. Then 4 gram of  $MgSO_4 \cdot H_2O$  and 1gram of NaCl was added, shaken for 5 minutes. Then added 1gram of sodium citrate dihydrate and 0.5 g of sodium hydrogen citrate sesquihydrate. The mixture was shaken vigorously for 1minute and then sonicated for 5 minutes followed by centrifugation for 10 minutes at 2000 rpm. 5 mL of the supernatant was taken and treated with 125 mg of PSA (primary secondary amine) and 750 mg of  $MgSO_4 \cdot H_2O$ , shaken for five minutes and then sonicated for 5 minutes and centrifuged again. Then supernatant clean liquid was collected in 50 mL round bottom flask and evaporated to dryness at 40 °C and 200 mbar in Rotavapor. Residue was reconstituted in 5 mL acetonitrile. 100  $\mu$ L of this were mixed with 1.9 mL PB so as to convert it to a 5 ppb pesticide solution in 5 % acetonitrile. The % inhibition of sensor response upon incubation in this solution for one hour was measured and the ppb was calculated using the corresponding calibration curve. The method was repeated thrice for each pesticide. The results obtained are shown in table 3.1.

**Table 3.1:** Biosensor recovery study

Pesticide	Initial Fortification Level	Expected ppb in 5% acetonitrile	ppb found	Recovery %	Mean recovery %	RSD (%)
Paraoxon	100	5	5.7	114	114	5.26
	100	5	6	120		
	100	5	5.4	108		
Carbofuran	100	5	5.2	104	102.67	4.06
	100	5	4.9	98		
	100	5	5.3	106		

Results show slightly higher recoveries in the two cases. Increase in recovery is more in case of paraoxon than carbofuran. The high recovery is attributed to Relatively higher recovery in case of paraoxon is attributed to under estimation of the true value in PB solution than in acetonitrile due to better solubility in the later.

### 3.5 Comparison with other AChE based biosensors

**Table 3.2:** Comparison of the different parameters of the sensor with the surface immobilized PPy-AChE sensors.

Electrode type	Chemicals used for fabrication	Storage stability	Reusability	Inhibition time	Reactivation time	LOD ppb/pesticide	Ref.
AChE-Au-PPy/GCE	Pyrrole, LiClO <sub>4</sub> , HClO <sub>4</sub> , HAuCl <sub>4</sub> , AChE	30 days<	-----	12min	10min	2(methyl parathion)	17
AChE/PAn-PPy-MWCNTs/GCE	Pyrrole, Aniline, HNO <sub>3</sub> , H <sub>2</sub> SO <sub>4</sub> , MWCNTs, SDS, AChE	30 days	-----		8 min	1(malathion)	4
PPy-AChE-Geltn- Glut/Pt	Pyrrole, Gelatin, Gluter-aldehyde, AChE	120 days	8assays. Above 70% residual activity	60 min	30 min	1.1(Paraoxon) 0.12(Carbofuran)	Present work

**Table 3.3:** Comparison of the analytic performance of the sensor with few of the contemporary AChE sensors when applied to the same analyte.

Analyte	Electrode	LOD(ppb)	Linear range(ppb)	Ref.
Carbofuran	AChE/Nafion/BSA/CoPC-SPE	0.06	0.022-22	29
	AChE-TCNQ/SPE	1.1	-----	30
	AuNP/AChE/Au	7.26	-----	31
	PPy/AChE-Gelatin/Pt	0.12	0.025-2, 5-60	Present work
Paraoxon	AChE/Fe <sup>3+</sup> -BSA-Nafion/SPE	10	14-173	23
	AChE/PAN-AuNPs/Pt	0.739	0.1-100	32
	AChE/Geltn-Cellulose/SPE	7975	-----	33
	AChE-Carbon Paste/Cu	0.86	0-33	34
	PPy-AChE-Geltn-Glut/Pt	1.1	0.1-12.5, 12.5-150	Present work

### 3.6 Conclusions

We have developed a novel, simple and highly sensitive method of fabrication of acetylcholinesterase biosensor for OP and OC pesticides. The method involves electro entrapment of the enzyme AChE in polypyrrole in presence of very low amount of supporting electrolyte (KCl) followed by cross linking with glutaraldehyde and gelatin. Apart from the relatively longer analysis time, the other parameters of the sensor such as the sensitivity, stability, reproducibility, reusability and the ease of fabrication are very excellent and promising ones. The fabrication method of the present biosensor is a 'green' one, particularly because, it does not involve the use of any nano particles, which are hazardous to the environment. Through this work we have demonstrated for the first time that polypyrrole amplifies the amperometric signal of thiocholine oxidation and lowers its oxidation potential from 0.7 V to 0.1 V. We have also demonstrated that gelatin and glutaraldehyde mixture can enhance the stability of the electro entrapped biosensors by providing a better cross linking than what was obtained earlier through mere use of glutaraldehyde.

---

**References**

1. Sotiropoulou, S., et al. *Biosens. Bioelectron.* **20**, 1674--1679, 2005.
2. Kandimalla, V. B., & Ju, H.X. *Chem. Eur. J.* **12**, 1074--1080, 2006.
3. Anitha, K., et al. *Biosens. Bioelectron.* **20**, 848--856, 2004.
4. Du, D., et al. *Biosens. Bioelectron.* **25**, 2503--2508, 2010.
5. Lin, Y., et al. *Electroanalysis* **16**, 145--149, 2004.
6. Gong, J.M., & Lin, X.Q. *Microchem. J.* **75**, 51--57, 2003.
7. Jeanty, G., et al. *Anal. Chim. Acta*, **436**, 119--128, 2001.
8. Liu, G., & Lin, Y. *Anal. Chem.* **78**, 835--843, 2006.
9. Lee, H.S., et al. *Chemosphere* **46**, 571--576, 2002.
10. Kindervater, R., et al. *Anal. Chim. Acta* **234**, 113--117, 1990.
11. Cosnier S., *Biosens. Bioelectron.* **14**, 443--456, 1999.
12. Mu, S., et al. *Synth. Met.* **88**, 249--254, 1997.
13. Ramanavicius, A., et al. *Electrochim. Acta* **51**, 6025--6037, 2006.
14. Fortier, G., et al. *Biosens. Bioelectrons.* **5**, 473--490, 1990.
15. Njagi, J., & Andreescu, S. *Biosens. Bioelectron.* **23**, 168--175, 2007.
16. Narlı, I., et al. *Anal. Chim. Acta* **572**, 25--31, 2006.
17. Gong, J., et al. *Biosens. Bioelectron.* **24**, 2285--2288, 2009.
18. Liu, G., et al. *Electrochem. Commun.* **7**, 1163--1169, 2005.
19. Ellman, G.L., et al. *Biochem. Pharmacol.* **7**, 88--95, 1961.
20. Dong, S., et al. *Analyst* **113**, 1525--1528, 1988.
21. Cadogan, A., et al. *Talanta* **39**, 617--620, 1992.

22. Vakurov, A., et al. *Biosens. Bioelectron.* **20**, 1118--1125, 2004.
23. Suprun, E., et al. *Anal. Bioanal. Chem.* **383**, 597--604, 2005.
24. Ramanavičius, A., et al. *Sens. Actuat. B* **111-112**, 532--539, 2005.
25. Kok, F.N., et al. *Biosens. Bioelectron.* **17**, 531--539, 2002.
26. Laane, C., et al. *Biotechnol. Bioeng.* **30**, 81--87, 1987.
27. Valdés Ramírez, G., et al. *Anal. Bioanal. Chem.* **392**, 699--707, 2008.
28. Lehotay, S., et al. *The J. AOAC.Int.* **88**, 595--614, 2005.
29. Laschi, S., et al. *Enzyme Microb. Tech.* **40**, 485--489, 2007.
30. Bucur, B., et al. *Anal. Chim. Acta* **562**, 115--121, 2006.
31. Shulga, O., & Kirchoff, J.R. *Electrochem. Commun.* **9**, 935--940, 2007.
32. Marinov, I., et al. *J. Mol. Catalysis B* **62**, 67--75, 2010.
33. Pohanka, M., et al. *Int. J. Electrochem. Sci.* **7**, 50--57, 2012.
34. Tuoro, D. D., et al. *New Biotechnology* **29**, 132--138, 2011.